Journal of Sound and Vibration 408 (2017) 1–19

Contents lists available at ScienceDirect

Journal of Sound and Vibration

journal homepage: www.elsevier.com/locate/jsvi

Fundamentals of active shielding based on implicit control

Ricardo Quintana [a,*], Yiu Lam [b], Diego Patino [a]

[a] Departamento de Electrónica, Pontificia Universidad Javeriana, Colombia
[b] School of Computing, Science & Engineering, University of Salford, United Kingdom

ARTICLE INFO

Article history:
Received 23 September 2016
Received in revised form
10 May 2017
Accepted 5 July 2017
Handling Editor: J. Lam

Keywords:
Active noise control
Active shielding
Implicit control
Finite difference method

ABSTRACT

Active noise control is a methodology to attenuate low frequency noise. The attenuation is usually achieved near the sensor which is used in the controller. In order to achieve the desired attenuation inside a desired zone without locating a sensor inside, a method called active shielding can be used. It works by controlling the pressure at boundaries of the desired zone. This article presents a novel method for implementing active shielding only using pressure sensors. It is based on a new concept called implicit control, which takes into account the locations of sensors. Some simulations validate the presented method for free fields.

1. Introduction

The active noise control is a methodology to attenuate the noise using the property of superposition. First approaches were published by Paul Leug and Coanda [1,2]. Specifically, the noise generated by a source is attenuated by adding another source which generates an “anti-noise” wave [3]. To produce an active attenuation, there are two schemes, feedback and feed-forward. They are differentiated because feed-forward scheme produces the control signal as a transformation of a reference signal of the emitted noise, while feedback scheme only uses information of acoustic pressure at the desired silent location through sensors. [4] is a review which depicts several issues in this field for both schemes.

In order to attenuate the pressure at a sensor location inside an enclosure, several algorithms have been created. Some of them are based on adaptive filters such as the filtered X Least Mean Squares (LMS) algorithm, Filtered U LMS algorithm, etc. [5]. Other algorithms are based on robust control theory, e.g. [6–9]. According to these references, these algorithms obtain an attenuation around 20 dB at the sensor location. A detailed description of these algorithms are found in [10], which is a review that includes nonlinear algorithms. However, the attenuation of the sound is only accomplished at or near the sensor location. Usually, the user, who is exposed to the noise, is not located at the sensor position. Inside enclosures with large volume, the mentioned ANC systems only control the noise at locations near the sensors. In order to increase the silent zone (locations where the noise is attenuated), multichannel control have been used [11,12].

Let's center the attention in the case that sensors cannot be located at the position of the users. Then, increasing the silent zone without using microphones at the user locations is a problem mentioned by several authors. A solution was proposed in [13], where an optimization problem is suggested. This mentions the possibility to optimize the sound pressure using the sensors and actuators (also called secondary sources) as optimization variables. A similar procedure is applied in

* Corresponding author.
E-mail address: rquintana@javeriana.edu.co (R. Quintana).

http://dx.doi.org/10.1016/j.jsv.2017.07.006
0022-460X/

[14], but it applies two consecutive optimization stages. The first stage takes into account only the sources positions, and the second the sensor locations. This can be applied using a simulation of the room. Thus, the sources and sensors are located optimally where the simulation results indicate.

Increasing the silent zone is possible by estimating the pressure at a desired location. It is known as virtual sensing. This method is carried out by first measuring the sound pressure at a different location. This signal is then transformed to obtain an approximation of the pressure at a desired location to be used as the error signal. The first algorithm was called virtual microphone arrangement [15]. It takes into account the sound pressure measured by a sensor. Its limitation is due to the assumption that the sound pressure generated by the noise sources is equal for the virtual and real sensor locations (desired and measured locations respectively). A modification called remote microphone [16] applies the same concept. However, it uses a transformation of the estimation of primary noise to avoid the assumption that the sound pressure components generated by the primary source are equal at both locations, and this transformation is not determined if it is not causal. [17] uses a Kalman filter as the estimator of the pressure, which also needs to establish a model of the system. Another proposal is based on the correlation of the pressure at different locations [18], but it is limited by the distance between real and virtual sensors. [19] introduces a nonlinear estimation to solve the problem of the non-causality relation between the measured and estimated pressure. The solution is a modification of the remote microphone algorithm. Other algorithms have been presented but only applied to one dimensional or not enclosed systems e.g. [20–22]. [23] deals with the problem that attenuating the noise using high number of virtual sensors requires high computational cost. Another issue is that the estimation is carried out using a sensor, but the real receiver is a human, which can produce a change on the estimation. To solve it, [24] proposes an approximation of a mathematical model of the identification system by using a head and torso simulator instead of human ears in the experiment.

Another important methodology for active control of sound field in a discrete region is active shielding. It works on the principle of boundary control with actuators on the boundary surface using information gathered from sensors on the boundary surface. The method developed by Jessel and Mangiante [25] and Canevet [26], known as the JMC method, uses Huygens' principle to formulate control of sound field in a zone with secondary sources on the boundary. Pressure and velocity detectors and monopole and dipole actuators are generally required to facilitate the sound field control [27]. Active shielding can also be derived from a formulation of Kirchhoff-Helmholtz integral equation [28]. In this case, only pressure sensors and monopole actuators are required, but the formulation suffers from the integral equation's inherent failure at the characteristic frequencies of the interior region [29]. Munjal and Erikson developed another approach based on electro-acoustic analogies, but it is limited by sensor position. It cannot be located at the same position as that of a node [30]. These active shielding approaches seek to minimize the total sound pressure (noise) in the region. In some cases, it may be possible to use directional measurements to separate the unwanted and wanted sound components in the region [31], but such application is limited since in most realistic cases the wanted component cannot be completely separated out by directional measurement alone. The method of using generalized Calderon's potentials and boundary projection operators [32], and the discrete formulation based on difference potentials [33–36], are a general class of active shielding methods that has the advantage of automatically preserving wanted sound in the region while attenuating unwanted sound coming into the region. However, similar to the JMC method, these approaches have the disadvantage of requiring both pressure and velocity sensors on the boundary surface to guarantee a universal solution. As demonstrated in [33,34], both monopole and dipole sources were also required to successfully realize the active shielding in practice. The method developed in this paper aims to avoid the additional cost and complexity of including velocity sensors and dipole control sources, and as a consequence it will sacrifice the generality of automatically preserving wanted sound in the shielded region.

Recently, an active shielding was applied also based on virtual sensing for a cylindrical shell [37], which is a method restricted to cylindrical shape and include the problems of virtual sensing. From these methods in active shielding, it is important to remark that they have a limitation. All of them produces a solution and not a control algorithm. In order to make the control system more robust, it is desired to obtain a feedback control [38].

This paper deals with the attenuation of noise of a zone inside a microphone array. The solution is a novel active shielding method which reduces the hardware complexity respect to virtual sensing methods because it avoids the estimation process. Furthermore, it only uses pressure sensors, instead of the particle velocity sensors. Regarding the limitation of other active shielding systems proposed in state of the art, this article shows that it can use any controller based on an optimization process to obtain the attenuation inside the silent zone (see the controller in Appendix B, which is the solution obtained for algorithms similar to the FxLMS). Moreover, this result is differentiated by an analysis that includes the time variable. It is based on the wave equation instead of Helmholtz equation.

This article is divided as follows: the next section defines the concept called implicit control. This concept is used to propose a novel method for active shielding in Section 3. In Section 4, several simulations validate the active shielding method. Furthermore, a comparison between virtual sensing and the proposed active shielding method is carried out in Section 5. Finally, some conclusions are given in Section 6.

2. Implicit control

Before understanding how the proposed active shielding system works, it is necessary to define a new concept:

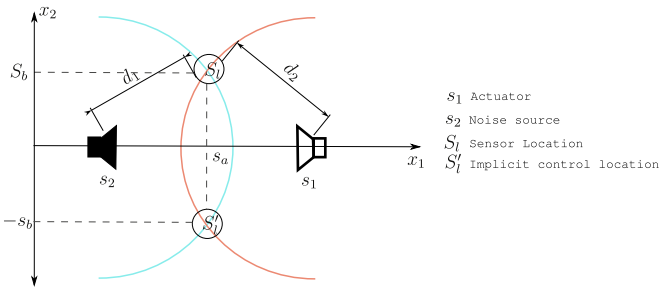

Fig. 1. Scheme of implicit control example for a 2D acoustic system.

Definition 2.1. Implicit control: It is the phenomenon that obtaining a specific value of variable implies getting a desired value for another variable.

For active noise control, it occurs when attenuating (controlling) the pressure at the sensor location, implies the attenuation at other location. It is important to remark that the pressure at each location is defined as a different variable. The aim of this new concept is to be applied as a method to ensure that attenuating the boundaries of a desired silent zone, any location inside it is also attenuated.

In order to clearly show this concept, an example of an active noise control system in two dimensional free field is taken into account. See the locations in the scheme in Fig. 1. The figure shows two point sources, one generates the noise and the other is the actuator (controlled source). They are located at $s_1 = [A_{1,a}, 0]$ and $s_2 = [A_{2,a}, 0]$ respectively (for the axis $[x_1, x_2]$). The sensor is located at $S_l = [s_a, s_b]$ (Location which is the pressure to be controlled) with a distance d_1 and d_2 from the noise source and actuator respectively. As additional restriction $A_{1,a} < s_a$ and $A_{2,a} > s_a$. Additionally, a location S'_l is defined as the point where the distance to both sources is equal to the distance between S_l and the sources.

The total pressure $p_t(x, t)$, at $x = [x_1, x_2]$ and time instant t, location can be expressed as a function of the pressure components $p_1(x, t)$ and $p_2(x, t)$, which represent the pressure due to the noise source s_2 and the actuator s_1 respectively. Then, it can be expressed as:

$$p_t(x, t) = p_1(x, t) + p_2(x, t) \tag{1}$$

For the frequency analysis of this case, these two components of pressure can be expressed as functions of distance d_1 or d_2 between the receiver at location S_l and the source s_1 or s_2 respectively, i.e.:

$$p_1(S_l, t) = j\rho_0 c \frac{Q_1 \eta}{4\pi d_1} e^{j(\omega t - \eta d_1)} \tag{2}$$

$$p_2(S_l, t) = j\rho_0 c \frac{Q_2 \eta}{4\pi d_2} e^{j(\omega t - \eta d_2)} \tag{3}$$

where ρ_0 is the air density; c is the speed of sound; Q_1 and Q_2 are the source strength; η is the wave number; and ω is the frequency of sound.

Furthermore, the control of the pressure at S_l is achieved if $p_t(S_l, t) = 0$. It means $p_1(S_l, t) = -p_2(S_l, t)$. This condition is accomplished from (1)–(3) if:

$$Q_2 = -\frac{Q_1 d_2}{d_1} e^{j(\eta d_2 - \eta d_1)} \tag{4}$$

Notice that Q_2, $p_1(S_l, t)$ and $p_2(S_l, t)$ only depend on the distances d_1 and d_2 due to ρ_0, c and η, which are constants. Hence, Eq. (4) is a solution for any other location S'_l such that the distance between the sources and S'_l are equal to S_l, eg. $S'_l = [s_a, -s_b]$ and both locations have the same value of pressure. It means that the implicit control occurs and controlling the pressure at S_l implies to control the pressure at S'_l because the attenuation of the pressure at one location implies the attenuation at the other location.

As a consequence of the implicit control phenomenon, a related issue appears:

Problem 1. How to find the locations to be controlled in order to obtain implicit control in a desired silent zone?

From the definition of implicit control, the issue is to find a set of locations $x_{1,s}, x_{2,s}, \ldots, x_{N,s}$ such that they achieve the implicit control at another set of locations $x_{i,r}$, with $i = 1,\ldots,M$ where M is the number of locations where the implicit control occurs. Defining two vectors with the pressure in frequency space for these locations as $P(\omega) := [F(p_t(x_{1,r}, t)), F(p_t(x_{2,r}, t)), \ldots, F(p_t(x_{M,r}, t))]$; $F(\cdot)$ is the Fourier transform and $\bar{P}(\omega) := [F(p_t(x_{1,s}, t)), F(p_t(x_{2,s}, t)), \ldots, F(p_t(x_{N,s}, t))]$, it is evident that the implicit control can be proven for locations that achieve the following condition:

$$\left\{ P(\omega) = G(\omega)\bar{P}(\omega) \right\} \text{ and } \bar{P}(\omega) \text{ is controlled} \tag{5}$$

where $G(\omega)$ is any linear transform.

For the example in Fig. 1, the Eq. (4) ensures the restriction (5) for $[x_{1,s} = S_l]$, $[x_{1,r} = S'_l]$ and $G(\omega) = 1$. Hence, the implicit control is accomplished in the case of Fig. 1.

3. Active shielding based on implicit control

According to [34], active shielding is a method where an "area involves a given region of space (bounded or unbounded) to be shielded from unwanted external noise by the active controls. The controls establish an active boundary, shielding the region from the noise".

This section describes a novel methodology to implement an active shielding system based on implicit control. It means obtaining a controller which produces a desired silent zone using the information of the pressure at its boundaries instead the pressure inside the silent zone with the concept shown in the previous section. Basically, the aim is to solve the Problem 1 with a set of pressure at boundaries $\bar{P}(\omega)$. For sake of simplicity, the analysis will be carried out in a two dimensional free field system. The procedure consists of discretizing the wave equation through the finite difference method. It allows the description of the pressure at one location as a function of the pressure at contiguous locations. Thus, the relation of the pressure inside the silent zone and its boundary can be written as a space state model (This is a general form to write equations which describes linear systems, see [38] for a more detailed description), which ensures a linear relationship between them and the restriction (5). Considering a desired silent zone where this zone can be discretized at locations $x_{i,j} = [x_i, x_j]$, with $i = 1,\ldots,I$, $j = 1,\ldots,J$, $x_{i+1,j} = [x_i + \Delta_x, x_j]$ and $x_{i,j+1} = [x_i, x_j + \Delta_x]$, the next statement can be proven:

Theorem 1. *The relation between the pressure at all discrete locations inside the desired silent zone $z_{2D}(k) \in \mathbb{R}^{IJ}$ and the pressure at the discrete locations at its boundaries $u_{2D}(k) \in \mathbb{R}^{2I+2J}$ is linear and can be written as a space state model of the form*:

$$\begin{bmatrix} z_{2D}(k+1) \\ z_{2D}(k) \end{bmatrix} = \begin{bmatrix} A_{2D} & \hat{A}_{2D} \\ \mathbb{I}_{IJ} & \mathbb{O}_{IJ,IJ} \end{bmatrix} \begin{bmatrix} z_{2D}(k) \\ z_{2D}(k-1) \end{bmatrix} + \begin{bmatrix} B_{2D} \\ \mathbb{O}_{IJ,2I+2J} \end{bmatrix} u_{2D}(k) \tag{6}$$

where A_{2D}, $\hat{A}_{2D}$ and B_{2D} are real matrices; $\mathbb{I}_{IJ}$ is an identity matrix with size $IJ \times IJ$; and $\mathbb{O}_{IJ,IJ}$ is a zero matrix with size $IJ \times IJ$. It means, this relation achieves the restriction (5).

Proof. Let us begin describing the behavior of pressure using the damped wave equation:

$$\nabla_{2D}(\, p(x,\, t)) - d\frac{\partial p(x,\, t)}{\partial t} - \frac{1}{c^2}\frac{\partial^2 p(x,\, t)}{\partial t^2} = 0 \tag{7}$$

where $\nabla_{2D}(\cdot) := \frac{\partial^2 \cdot}{\partial x_1^2} + \frac{\partial^2 \cdot}{\partial x_2^2}$ and d is the damping coefficient.

Using this continuous time equation, it is quite complex to express the pressure in the desired area based on the pressure at other locations. Hence, Eq. (7) is discretized using the finite difference method. Specifically, the differential operator is approximated by:

$$\frac{\partial p(x_{i,j},\, t)}{\partial t} \approx \frac{p(x_{i,j},\, (k+1)\Delta_t) - p(x_{i,j},\, (k-1)\Delta_t)}{2\Delta_t} \tag{8}$$

$$\frac{\partial^2 p(x_{i,j},\, t)}{\partial t^2} \approx \frac{p(x_{i,j},\, (k+1)\Delta_t) - 2p(x_{i,j},\, k\Delta_t) + p(x_{i,j},\, (k-1)\Delta_t)}{\Delta_t^2} \tag{9}$$

$$\frac{\partial^2 p(x_{i,j},\, t)}{\partial x_1^2} \approx \frac{p(x_{i+1,j},\, t) - 2p(x_{i,j},\, t) + p(x_{i-1,j},\, t)}{\Delta_x^2} \tag{10}$$

$$\frac{\partial^2 p(x_{i,j},\, t)}{\partial x_2^2} \approx \frac{p(x_{i,j+1},\, t) - 2p(x_{i,j},\, t) + p(x_{i,j-1},\, t)}{\Delta_x^2} \tag{11}$$

where Δ_t is the sample time. In order to simplify the notation, $p(x_{i,j},\, k\Delta_t) =: p(x_{i,j},\, k)$, it implies $t = k\Delta_t$. Regarding the approximation using finite difference method, it is valid when the variation of the pressure is low with respect to its variations in space. It implies that higher values of Δ_x produces high error and this approximation is not valid. Specifically, this discretization applied to the discrete model of the wave equation has been analyzed for $d = 0$, e.g. [39] studies when the model is unstable and [40] deals with the phenomenon called dispersion. However, for $d \neq 0$, it is not analyzed. In this paper, a statistical analysis of the behavior of this limitation in active shielding method is carried out and presented in Section 4.3.

Using these definitions and approximations, the pressure at a discrete location can be written as:

$$p(x_{i,j},\, k+1) = \gamma_{2,a}\left[p(x_{i-1,j},\, k) + p(x_{i+1,j},\, k) + p(x_{i,j-1},\, k) + p(x_{i,j+1},\, k)\right] + \gamma_{2,b}\,p(x_{i,j},\, k) + \gamma_{2,c}\,p(x_{i,j},\, k-1) \tag{12}$$

With:

$$\gamma_{2,a} = \frac{2c^2\Delta_t^2}{\Delta_x^2\left(dc^2\Delta_t + 2\right)} \tag{13}$$

$$\gamma_{2,b} = \left[\frac{4\left(\Delta_x^2 - 2c^2\Delta_t^2\right)}{\Delta_x^2\left(dc^2\Delta_t + 2\right)}\right] \tag{14}$$

$$\gamma_{2,c} = \left[\frac{dc^2\Delta_t - 2}{\left(dc^2\Delta_t + 2\right)}\right] \tag{15}$$

It is important to remark that Eq. (12) produces a set of equations for different values for i and j. For example, for $i = 1, 2$ and $j = 1$:

$$p(x_{1,1},\, k+1) = \gamma_{2,a}\left[p(x_{0,1},\, k) + p(x_{2,1},\, k) + p(x_{1,0},\, k) + p(x_{1,2},\, k)\right] + \gamma_{2,b}\,p(x_{1,1},\, k) + \gamma_{2,c}\,p(x_{1,1},\, k-1) \tag{16}$$

$$p(x_{2,1},\, k+1) = \gamma_{2,a}\left[p(x_{1,1},\, k) + p(x_{3,1},\, k) + p(x_{2,0},\, k) + p(x_{2,2},\, k)\right] + \gamma_{2,b}\,p(x_{2,1},\, k) + \gamma_{2,c}\,p(x_{2,1},\, k-1) \tag{17}$$

According to [38], the relation exposed in Eq. (5) has an analogous relation in a space state model. It means, writing Eq. (12) for any i and j inside the desired silent zone as a space state model is enough to ensure the relationship in Eq. (5). Assuming the silent zone is a square, the next procedure shows how to obtain the desired model.

First, the pressures of discrete locations inside the desired silent zone form a vector. In order to organize this vector, a set of pressures along a line (for a fixed value of j) produces a vector as follows:

$$\dot{z}_j(k) := [p(x_{1,j},\, k),\, p(x_{2,j},\, k),\, \ldots,\, p(x_{I,j},\, k)]^T \tag{18}$$

The vector $\dot{z}_j(k)$ contains the pressures at the locations inside red rectangles in Fig. 2. Each value of j produces a vector and a rectangle in the Fig. 2. These vectors $\dot{z}_j(k)$ are concatenated as:

$$z_{2D}(k) := [\dot{z}_1(k)^T \dot{z}_2(k)^T \cdots \dot{z}_J(k)^T]^T \tag{19}$$

Thus, the vector $z_{2D}(k)$ is the analogous to $P(\omega)$ in discrete time space.

On the other hand, the vector of pressures at locations of the boundary of desired silent zone is formed as:

$$\dot{u}_a(k) := [p(x_{1,0},\, k),\, p(x_{2,0},\, k),\, \ldots,\, p(x_{I,0},\, k)]^T \tag{20}$$

$$\dot{u}_b(k) := [p(x_{1,J+1},\, k),\, p(x_{2,J+1},\, k),\, \ldots,\, p(x_{I,J+1},\, k)]^T \tag{21}$$

$$\dot{u}_c(k) := [p(x_{0,1},\, k),\, p(x_{0,2},\, k),\, \ldots,\, p(x_{0,J},\, k)]^T \tag{22}$$

$$\dot{u}_d(k) := [p(x_{I+1,1},\, k),\, p(x_{I+1,2},\, k),\, \ldots,\, p(x_{I+1,J},\, k)]^T \tag{23}$$

$$u_{2D}(k) := [\dot{u}_a(k)^T,\, \dot{u}_b(k)^T,\, \dot{u}_c(k)^T,\, \dot{u}_d(k)^T]^T \tag{24}$$

Each vector of $\dot{u}_a(k)$, $\dot{u}_b(k)$, $\dot{u}_c(k)$ and $\dot{u}_d(k)$ take the pressures of the locations inside each green rectangle in Fig. 2. Hence,

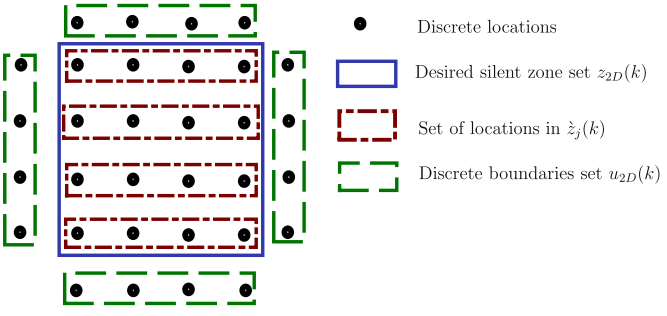

Fig. 2. Scheme of active shielding system for two dimensional space. (For interpretation of the references to color in this figure, the reader is referred to the web version of this article).

$u_{2D}(k)$ contains the pressure at all the discrete locations at the boundaries of the silent zone and is analogous to $\bar{P}(\omega)$. According to Eq. (12), $z_{2D}(k)$ is a linear function of $u_{2D}(k)$ and its own past values. It means that the following system of linear equations based on Eq. (6) can be written to obtain $z_{2D}(k)$.

$$z_{2D}(k+1) = A_{2D} z_{2D}(k) + B_{2D} u_{2D}(k) + \hat{A}_{2D} z_{2D}(k-1) \tag{25}$$

Where the matrices A_{2D}, B_{2D} and $\hat{A}_{2D}$ are the relations between the vectors which are obtained from (12) and they are explained below:

- $\hat{A}_{2D}$: Eq. (12) expresses that $\gamma_{2,c}$ is the coefficient which relates the values of the pressure $p(x_{i,j}, k-1)$ with $p(x_{i,j}, k+1)$. In Eq. (25), these pressures are located in the vectors $z_{2D}(k+1)$ and $z_{2D}(k-1)$ respectively at the same position. As a consequence, the diagonal locations of the matrix $\hat{A}_{2D}$ are equal to $\gamma_{2,c}$ and zero at any other locations. Mathematically it is written as $\hat{A}_{2D} = \gamma_{2,c}\mathbb{I}_{IJ}$.
- A_{2D}: lets begin analyzing the relation between $\dot{z}_j(k+1)$ and $\dot{z}_j(k)$. In order to simplify the notation, a matrix A_{b2} is defined as the relation between these two vectors and it is a sub-block-matrix in A_{2D}. Its values depend on the pressures $p(x_{i,j}, k+1)$ and $p(x_{i,j}, k)$, which are at the position i inside the vectors $\dot{z}_j(k+1)$ and $\dot{z}_j(k)$. The relationship between these pressures is the multiplication of the constant $\gamma_{2,b}$ which is the value for the locations i, i of the matrix A_{b2}. Furthermore, the pressures $p(x_{i-1,j}, k)$ and $p(x_{i+1,j}, k)$ are also located in $\dot{z}_j(k)$ at positions $i-1$ and $i+1$, except if $i-1 \leq 0$ or $i+1 > I$ (this exception is for locations that are not inside the vector because they are out of the desired silent zone). Their relation with $p(x_{i,j}, k+1)$ is given by the constant $\gamma_{2,a}$ and it is the value for all locations i, $i-1$ and i, $i+1$ in the matrix A_{b2}. Hence, the matrix A_{b2} is:

$$A_{b2} := \begin{pmatrix} \gamma_{2,b} & \gamma_{2,a} & 0 & \cdots & \cdots & 0 \\ \gamma_{2,a} & \gamma_{2,b} & \gamma_{2,a} & 0 & & \vdots \\ 0 & \gamma_{2,a} & \gamma_{2,b} & \gamma_{2,a} & \ddots & \vdots \\ \vdots & 0 & \ddots & \ddots & \ddots & 0 \\ \vdots & & \ddots & \gamma_{2,a} & \gamma_{2,b} & \gamma_{2,a} \\ 0 & \cdots & \cdots & 0 & \gamma_{2,a} & \gamma_{2,b} \end{pmatrix} \tag{26}$$

Another relationship that needs to be taken into account is between $\dot{z}_j(k+1)$ and $\dot{z}_{j+1}(k)$. The pressure at position i in the vector $\dot{z}_j(k+1)$ is $p(x_{i,j}, k)$ which is related to $p(x_{i,j+1}, k)$ at the position i in $\dot{z}_{j+1}(k)$. Then, the matrix that relates these two vectors is $\gamma_{2,c}\mathbb{I}_I$. The same matrix relates the vectors $\dot{z}_j(k+1)$ and $\dot{z}_{j-1}(k)$. For these two cases, it is important to remark that they do not apply for $j-1 \leq 0$ and $j+1 > J$ (it only applies for the discrete locations inside the desired silent zone). Using this result and A_{b2}, the matrix A_{2D} can be constructed, due to the relationships between the vectors, as:

$$A_{2D} = \begin{pmatrix} A_{b2} & \gamma_{2,a}\mathbb{I}_I & \mathbb{O}_{I,I} & \cdots & & \cdots & \mathbb{O}_{I,I} \\ \gamma_{2,a}\mathbb{I}_I & A_{b2} & \gamma_{2,a}\mathbb{I}_I & \mathbb{O}_{I,I} & \ddots & & \vdots \\ \mathbb{O}_{I,I} & \gamma_{2,a}\mathbb{I}_I & A_{b2} & \gamma_{2,a}\mathbb{I}_I & \ddots & \ddots & \vdots \\ \vdots & \mathbb{O}_{I,I} & \ddots & \ddots & \ddots & \mathbb{O}_{I,I} & \vdots \\ \vdots & \ddots & \ddots & \ddots & \ddots & \ddots & \mathbb{O}_{I,I} \\ \vdots & & \ddots & \mathbb{O}_{I,I} & \gamma_{2,a}\mathbb{I}_I & A_{b2} & \gamma_{2,a}\mathbb{I}_I \\ \mathbb{O}_{I,I} & \cdots & \cdots & \cdots & \mathbb{O}_{I,I} & \gamma_{2,a}\mathbb{I}_I & A_{b2} \end{pmatrix} \tag{27}$$

- B_{2D} : as it was mentioned before, the relation between the silent zone and the boundary locations has not been analyzed yet. This is because it corresponds to the matrix B_{2D}. The vectors $\dot{z}_1(k+1)$ and $\dot{u}_a(k)$ contain the pressures $p(x_{i,1}, k+1)$ and $p(x_{i,0}, k)$ respectively. Thus, the relation between these vectors is given by the matrix $\gamma_{2,a}\mathbb{I}_L$. Notice that this matrix also relates the vectors $\dot{z}_I(k+1)$ and $\dot{u}_d(k)$ and it becomes a sub-block-matrix inside B_{2D} at two locations.
  On the other hand, $p(x_{1,j}, k+1)$ for $j = 1$–J. The first term in the vector $\dot{z}_j(k)$, is related by the constant $\gamma_{2,a}$ to $p(x_{0,j}, k)$, the pressures in $\dot{u}_b(k)$. Thus, the matrix that relates $\dot{z}_j(k)$ with $p(x_{0,j}, k)$ is:

$$b_{2D,1} := \begin{bmatrix} \gamma_{2,a} \\ 0 \\ \vdots \\ 0 \\ 0 \end{bmatrix} \tag{28}$$

The constant $\gamma_{2,a}$ also relates the pressure $p(x_{I,j}, k+1)$ for $j = 1$ to J. It means, the last location in vector $\dot{z}_j(k)$ is related to $p(x_{I+1,j}, k)$, which is located in the vector $\dot{u}_c(k)$. Following the same analysis to obtain $b_{2D,1}$, it is obtained the matrix which relates $\dot{z}_j(k)$ with $p(x_{I+1,j}, k)$.

$$b_{2D,2} := \begin{bmatrix} 0 \\ 0 \\ \vdots \\ 0 \\ \gamma_{2,a} \end{bmatrix} \tag{29}$$

The matrices $\gamma_{2,a}\mathbb{I}_L$, $b_{2D,1}$ and $\gamma_{2,a}$ are used to obtain B_{2D} as follows according to the locations of the vectors $\dot{z}_j(k+1)$, $\dot{u}_a(k)$, $\dot{u}_b(k)$, $\dot{u}_c(k)$ and $\dot{u}_d(k)$ in the vectors $z_{2D}(k+1)$ and $u_{2D}(k)$:

$$B_{2D} = \begin{bmatrix} \gamma_{2,a}\mathbb{I}_I & b_{2D,1} & \mathbb{O}_{I,2} & \cdots & \cdots & \mathbb{O}_{I,1} & b_{2D,2} & \mathbb{O}_{I,1} & \cdots & \cdots & \mathbb{O}_{I,1} & \mathbb{O}_{I,I} \\ \mathbb{O}_{I,I} & \mathbb{O}_{I,1} & b_{2D,1} & \cdots & & \vdots & \mathbb{O}_{I,1} & b_{2D,2} & \mathbb{O}_{I,1} & \cdots & \vdots & \vdots \\ & & \vdots & \ddots & & \vdots & & \vdots & \ddots & & \vdots & \vdots \\ \vdots & \vdots & & & b_{2D,1} & \mathbb{O}_{I,1} & \vdots & & & b_{2D,2} & \mathbb{O}_{I,1} & \mathbb{O}_{I,I} \\ \mathbb{O}_{I,I} & \mathbb{O}_{I,1} & \cdots & & \mathbb{O}_{I,1} & b_{2D,1} & \mathbb{O}_{I,1} & \cdots & & \mathbb{O}_{I,1} & \mathbb{O}_{2D,2} & \gamma_{2,a}\mathbb{I}_I \end{bmatrix} \tag{30}$$

Notice that the model (25) is now completed, and it can be rewritten as the space state model in Eq. (7). Thus, it is shown that the pressures in $z_{2D}(k)$ and $u_{2D}(k)$ can be related as input and output of a linear system which does not have additional inputs. It means the condition in Eq. (5) and Theorem 1 are achieved. Also, it shows that the pressures in $z_{2D}(k)$ are variables where the implicit control occurs when the pressures in $u_{2D}(k)$ are controlled. □

This also proves that controlling the noise at the boundaries of a desired square silent zone is a sufficient condition to control the noise inside this square. Furthermore, using a controller for the pressure at boundaries is an active shielding method because it does not need additional information, such as the pressure inside the desired silent zone. Additionally, the same procedure can be followed to obtain the result in a three dimensional system as shown in Appendix A.

Also, it is important to remark that Eq. (5) has a limitation when $G(\omega)$ has poles. Nevertheless, the Eq. (5) here does not have this limitation. This is because the Eq. (12) shows that the pressure at one location only depends on pressure of adjacent locations. For the desired silent zone, all of them are in vectors $z_{2D}(k)$ and $u_{2D}(k)$ and system in Eq. (6) becomes zero if it is stable and $u_{2D}(k)$ is a vector of zeros for all k. The values of matrices A_{2D} and $\hat{A}_{2D}$ affects stability. However, the conditions of stability are assumed because it is expected that, for any constant pressure at boundaries, the pressure inside does not increase to infinity. The proposed theory does have a disadvantage in comparison with active shielding based on Calderon's projection method [32] and discrete difference potentials method [33] when the boundary discrete locations coincide with pressure node locations. Those boundary projection methods use both pressure and velocity sensors, while the controllers in the proposed theory is based on pressure sensors alone, making it not possible to apply this method when the sensors are at pressure nodes. Specifically for the controller proposed in Appendix B, the inverse of matrix $(H^H(\omega)H(\omega))^{-1}$ cannot be calculated, $H(\omega)$ becomes a not full rank matrix. A deeper analysis of such cases will be considered for future work.

4. Validation

Towards validating analytically the proposed Theorem 1, several simulations will be carried out. The idea is taking benefit of the relation between the implicit control and the active shielding method. Therefore, using an active noise control system focused on the pressure at the boundaries, the desired silent zone is evaluated. This evaluation consists of examining the value of the attenuation, with respect to an emitted sinusoid noise signal. If it is higher than 10 dB, then it is considered satisfactory attenuation. If the whole desired silent zone achieves satisfactory attenuation, then it means that the implicit control is also achieved and the theory exposed in Section 3 is valid.It is important to remark that attenuation higher than 10 dB is not assumed to be 100% attenuation, but this is a common limit for a desired attenuation used by other authors, e.g. [41].

These simulations are based on the control method proposed in Appendix B. It implies the control signal is the optimum value to minimize the pressure at boundary locations.

4.1. Two dimensional system

In the two dimensional system, shown in Fig. 3, 408 noise sources have been taken into account in free field. They formed a circle with radius equal to 14 m. In the figure, this circle is shown in red. In the center of it, 12 actuators form a square with each side 12 m long and three actuators on each side. Each actuator is shown by a blue asterisk. A set of sensors forms

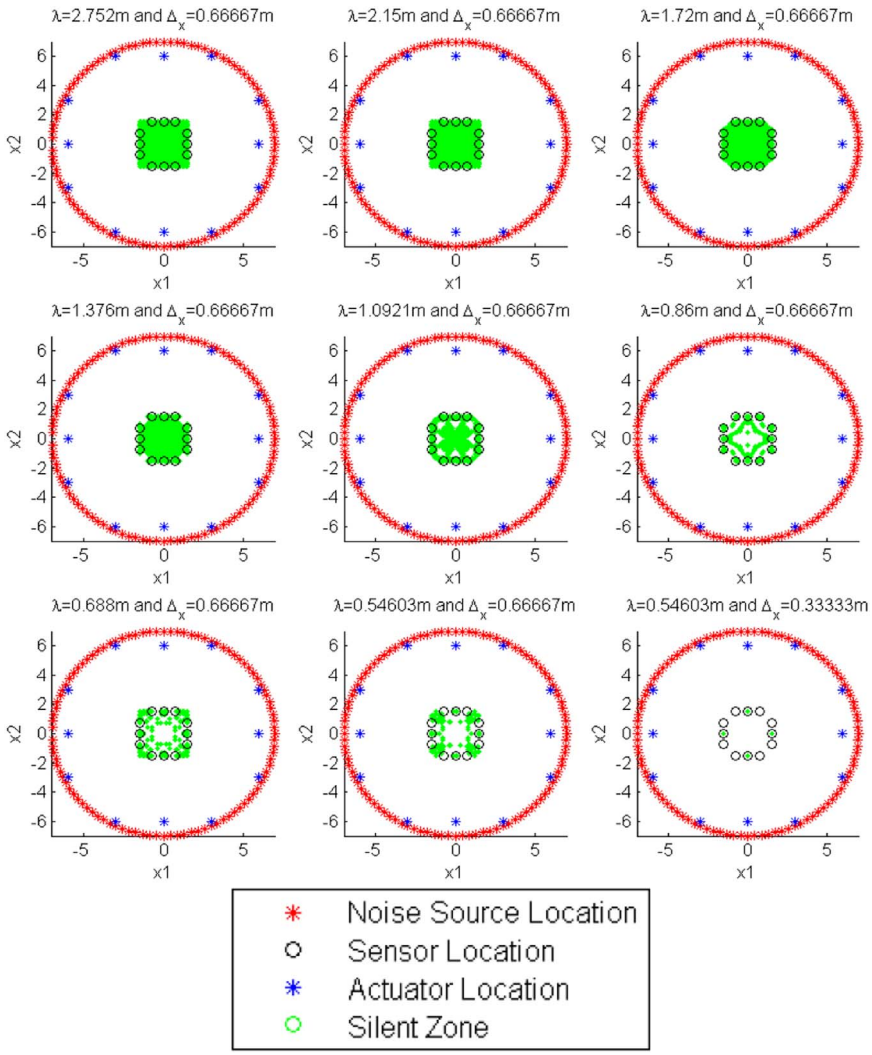

Fig. 3. Scheme of acoustic active shielding 2D system and its generated silent zone. (For interpretation of the references to color in this figure, the reader is referred to the web version of this article).

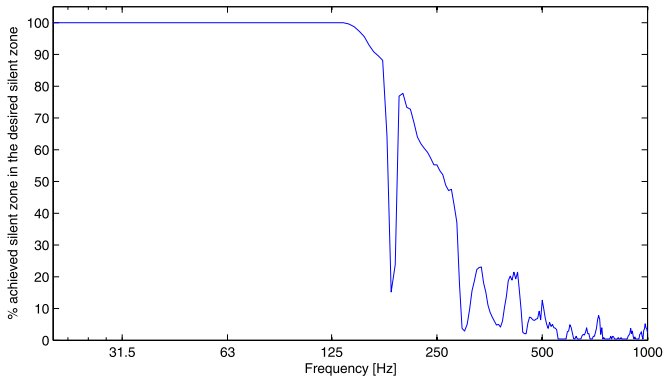

Fig. 4. Percent of the desired silent zone achieved with respect to the frequency in a two dimensional system.

another square with each of its sides 3 m long. Each location of this set is shown by a black small circle and their pressures form the vector $u_{2D}(k)$. There are 12 locations and represent the sensors of the control system. For this case, the control system is focused on minimized the square of pressure in the zone inside these 12 sensor locations. It is necessary to remark that for this case $I = J = 3$ and Δ_x is 0.75 m.

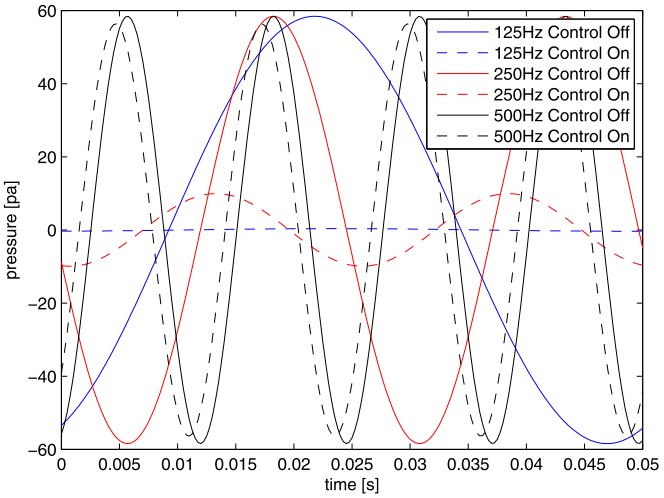

Fig. 5. Error signals simulated at center of silent zone for two dimensional system.

The attenuation is hard to be visualized for a total area, instead of that, the silent zone obtained is shown in green color. In Fig. 3, it is evident that the theory works well at low frequencies, at 100 Hz, 125 Hz and 160 Hz. For more detailed information, Fig. 4 shows the achieved percentage of the desired silent zones according to the frequency. It is evident, if the frequency is increased, the achieved silent zone decreases. At frequencies lower than 125 Hz, 100% of the silent zone is achieved. For higher frequencies, lower values of this percentage are obtained until less than 10% at 500 Hz. It implies that the attenuation decreases inside the silent zone when the frequency is increased. This decrease is not uniform and has troughs. These results show that implicit control is achieved for low frequencies, where it is expected to work according to the finite difference discretization. This is a limitation of the theoretical approach in previous section. The value of Δ_x, which is less than the wave length at 125 Hz (1.72 m), means that the theory is assured if Δ_x is lower than 1/3 of the wave length for this scheme. Thus, as the implicit control is achieved, this agrees with the Theorem 1.

In order to better explain local behavior inside the silent zone, the pressure at center of desired silent zone is simulated, see Fig. 5. There, it is shown the sinusoid signals noise for 125 Hz, 250 Hz and 500 Hz, when the control system is on and off. The pressures represented by continuous lines are without control and dotted line is with the influence of the controller. For all frequencies the noise is attenuated, but this attenuation varies with respect to the frequency. At low frequencies, the attenuation is higher, which agrees with the general behavior of the attenuation inside the whole silent zone.

4.2. Three dimensional system

After the simulations obtained using the two dimensional systems, the three dimensional system is also simulated (see the theory in the Appendix A). Analogous to the simulations in two dimensions, the three dimensional system replaces the circle of noise sources by a shell of a sphere with 14 m of radius and 114 sources, as it is shown in Fig. 6 in the part a. The squares are replaced by the shell of cubes of 54 locations each one. The biggest cubic shell in the figure (formed by dots in black color) locates the actuators. Each side of this cube is a square of 3×3 actuators, the size of each side of the squares is 12 m. The other cubic shell (formed by dots in blue color) contains the locations where the control is achieved. It is similar to the other cube, the only difference is the size of each side that is 3 m. The pressures of these locations are contained in $u_{3D}(k)$. For this case, also Δ_x is 0.75 m and $I = J = L = 3$.

The 3D results are very similar to the two dimensional system as they are shown in Fig. 6b. This figure shows a front view of the scheme with the generated silent zone. The frequencies of 100 Hz, 125 Hz and 160 Hz produce the target attenuation, but it cannot be achieved at higher frequencies. A more detailed analysis of the achieved silent zone is shown in Fig. 7. It confirms the high percent of the attenuation for the mentioned frequencies. However, at 160 Hz, 100% of the silent zone is not achieved. This silent zone is achieved at the frequencies lower than 125 Hz. In order to obtain the desired silent zone, it implies that Δ_x must be lower than 1/3 of the wave length.

The local behavior inside the silent zone is also evaluated at center of desired silent zone, see Fig. 8. There, the pressure sinusoid signals are shown for 125 Hz, 250 Hz and 500 Hz, when the control system is on and off. Again (as the two dimensional system), the pressures represented by continuous lines are without control and dotted line is with the influence of the controller. The pressure at center of desired silent zone has similar behavior to the whole silent zone, shown in Fig. 6. This means higher attenuation at low frequencies and lower at high frequencies. This result completely agrees with the two dimensional system and fits with the behavior shown in Fig. 7.

The results using a three dimensional system totally agree with the results for two dimensional system. They also lead in the direction of the theoretical approach of the Theorem 1, which is proven for three dimensional system in Appendix A.

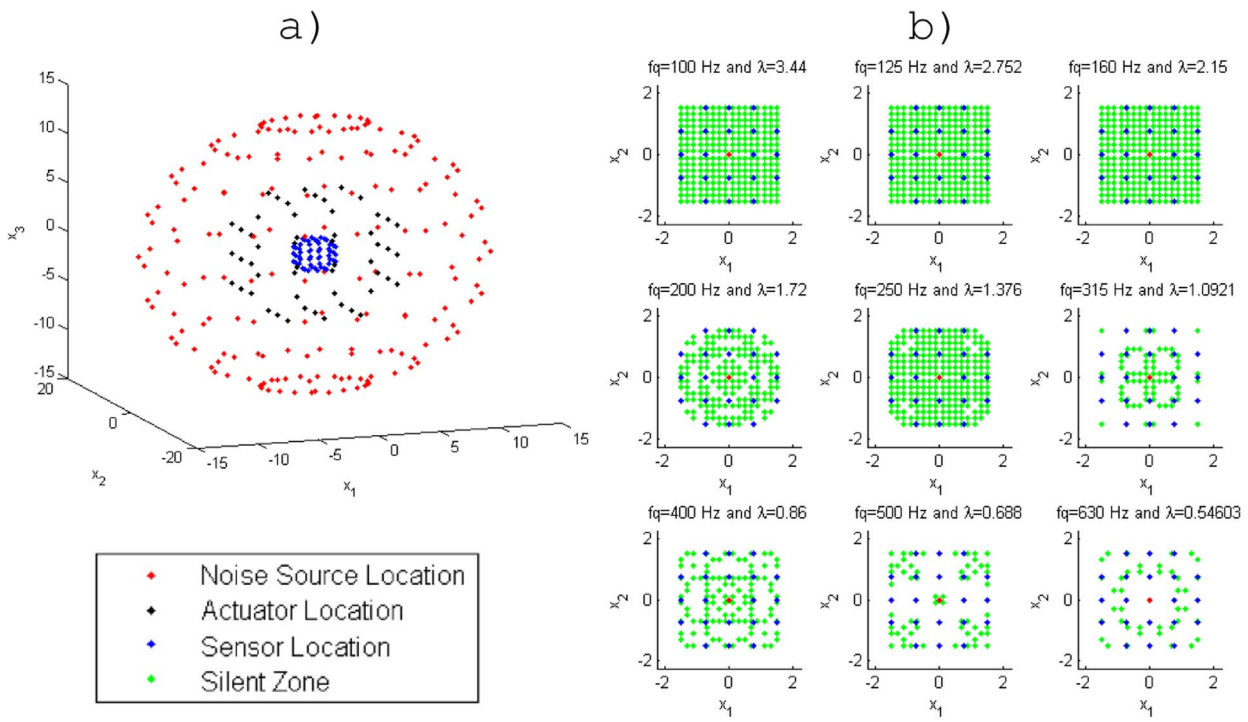

Fig. 6. Scheme of acoustic active shielding 3D system with the generated silent zone. a) Location of sensor, actuators and noise sources. b) Silent zone generated by frequency. (For interpretation of the references to color in this figure, the reader is referred to the web version of this article).

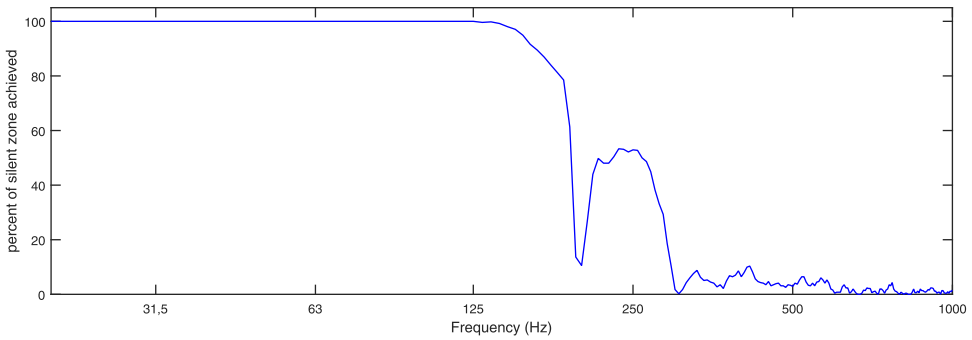

Fig. 7. Percent of the desired silent zone achieved with respect to the frequency in a three dimensional system.

4.3. The distance between control locations

According to previous simulations, one of the questions to be solved is: which value for Δ_x is valid to achieve the desired silent zone? Using similar simulations to those shown previously for two and three dimensional systems, different values of Δ_x are tested. Using a boundary formed by the sensors with the same length from previous simulations, the values of I, J and L are changed. This produces the variation for Δ_x. Also, this variation is evaluated for different frequencies and the parameter to compare the different cases is the percentage of area achieved of the desired silent zone.

For simulations with two dimensional and three dimensional systems, the Figs. 9 and 10 show the percentage of the desired silent zone which achieves the attenuation higher than 10 dB with respect to the relation between the distance Δ_x and the wave length λ. For all the frequencies and from both systems, the result produces the same performance. For low values of Δ_x/λ, the silent zone is not achieved because the controller produces undetermined mathematical operations. This controller needs to calculate the pseudo-inverse matrix of secondary paths, which is not possible when they are very similar. Hence, the sensors must be separated enough with respect to the wave length or the control signal cannot be calculated, for more information see Appendix B (This interval is not shown in Figs. 4 and 7 because it occurs at very lower frequency to be shown). As result, the attenuation is not obtained at the boundaries. Therefore, the implicit control is not achieved. This first interval is due to the controller, not to the proposed theory. In spite of it, this interval is taken into account to ensure completeness in the analysis. Then, according Figs. 9 and 10, there is an interval of values of Δ_x/λ where the control system

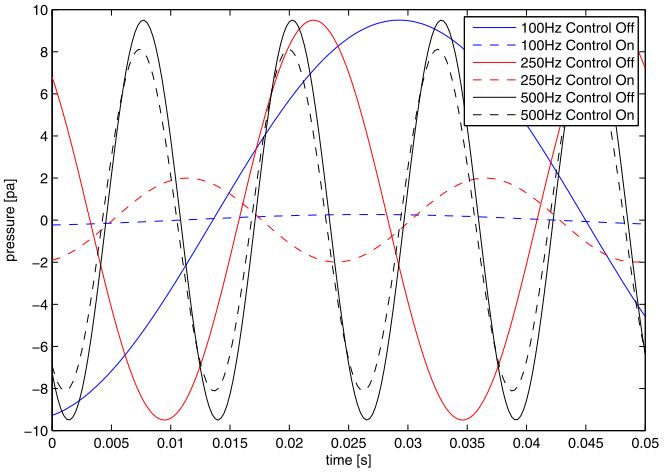

Fig. 8. Error signals simulated at center of silent zone for three dimensional system.

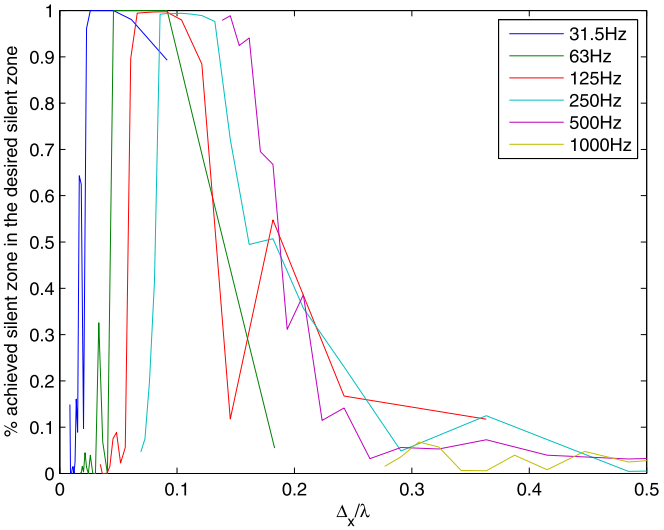

Fig. 9. Effectiveness of implicit control varying Δ_x and frequency for the 2D system.

obtains the complete silent zone. The second interval is explained due to the theory exposed in Theorem 1. Other values of Δ_x/λ produces an interval which shows that the attenuation is not achieved. This is when the implicit control is not achieved. The third interval is due to the limitation when the finite difference step is not sufficiently fine to discretize the wave equation. Moreover, it is important to remark on the variation of these intervals when the frequency also varies. For higher frequencies, the desired silent zone is obtained even for higher values of Δ_x/λ.

For a more detailed analysis, Figs. 11 and 12 plot the maximum and minimum values of Δ_x/λ where the 90% of the desired silent zone is achieved. In Fig. 11, these maximum and minimum values of Δ_x/λ are shown with respect to the frequency for the two dimensional system, while Fig. 12 shows the same information, but obtained using the three dimensional system. These figures also show the estimated models used to relate the parameters Δ_x/λ and the percentage of the achieved silent zone. For the estimated models, the next equations are proposed:

$$\zeta_M = \alpha_{M,1}(\ln(\omega)) + \alpha_{M,0} \tag{31}$$

$$\zeta_m = \alpha_{m,1}(\ln(\omega)^2) + \alpha_{m,0} \tag{32}$$

Where ζ_M and ζ_m are the maximum and minimum values of Δ_x/λ where the achieved silent is expected to be higher than 90% of the desired silent zone, $\alpha_{M,0}$, $\alpha_{M,1}$, $\alpha_{m,0}$ and $\alpha_{m,1}$ are coefficients obtained through an optimization process which minimizes the mean square error between the data obtained and their corresponding model. The values obtained for these coefficients are shown in the Table 1.

The most important result of this section is that there exists a relation between the frequency of the sound, Δ_x and the

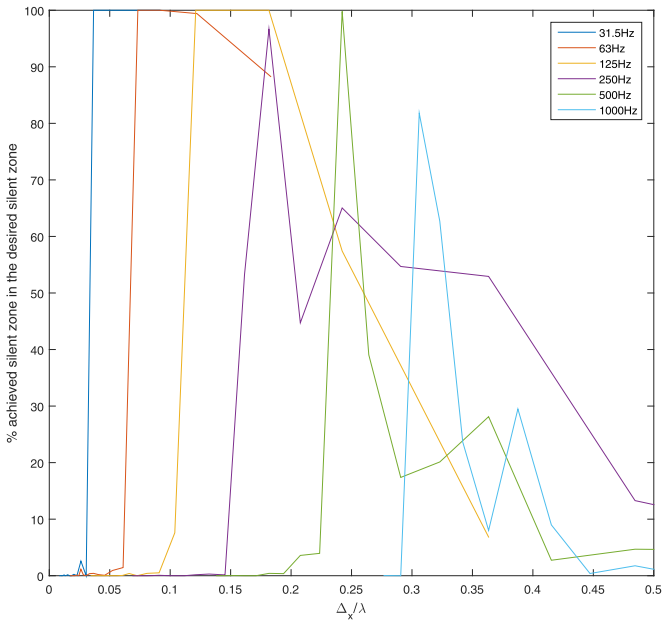

Fig. 10. Effectiveness of implicit control varying Δ_x and frequency for the 3D system.

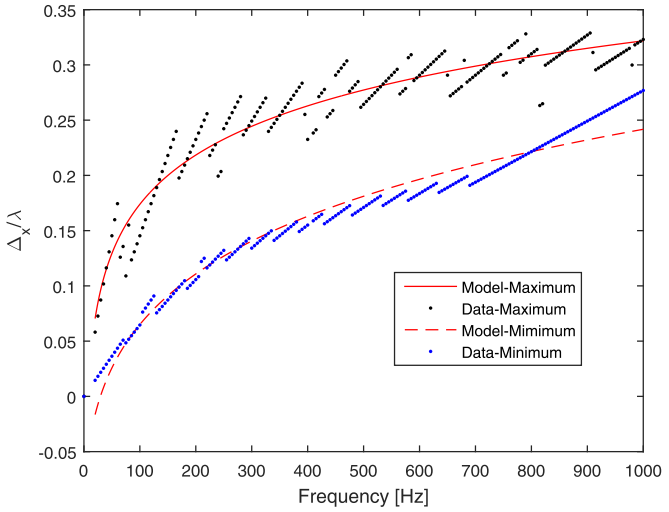

Fig. 11. Maximum and minimum values of Δ_x/λ where the active shielding method achieves 90% of the silent zone for a two dimensional system.

achieved silent zone. Additionally, this relation agrees with the case where the approximations (8)–(11) are expected to be valid. The Figs. 11 and 12 confirm this statement. Furthermore, this section obtains an Eq. (31) which describes the maximum relation Δ_x/λ to obtain the 90% of the desired zone while the controller attenuates the discrete boundaries.

5. Comparison between virtual sensing and active shielding

In this paper, the active shielding is proposed as an alternative solution for virtual sensing. Thus, a simulation between these two methodologies is carried out in this section. Here, it presents simulations for different frequencies using same locations for sensors and actuators for active shielding and virtual sensing. This comparison is carried out to show advantages of active shielding through an example. However, this is not conclusive, is just to show an example as a first step for future works.

For this simulation, it uses a similar scheme to the one proposed in Section 4.1. The results can be visualized in Figs. 13 and 14. 408 noise sources form a circle with 6 m of radius. The array of 12 actuators is the boundary of a square, which each side is a three meters line. The sensors are located forming the boundaries of another square with two meters side length. In

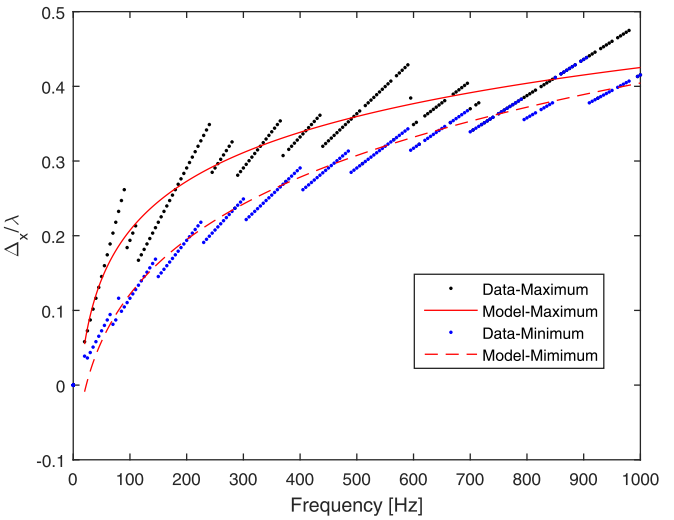

Fig. 12. Maximum and minimum values of Δ_x/λ where the active shielding method achieves 90% of the silent zone for a three dimensional system.

Table 1
Coefficient values of the mathematical models.

Coefficient	2D data	3D data
$\alpha_{M,0}$	0.0235	0.0224
$\alpha_{M,1}$	0.4727	0.2778
$\alpha_{m,0}$	−0.1220	−0.2288
$\alpha_{m,1}$	0.0642	0.0947

order to apply the virtual sensing method, the desired silent zone is full of a square of 5 × 5 virtual sensors (25 virtual sensors are located). The control signal for active shielding is the method in Appendix B. While, for virtual sensing, it is obtained using the optimum value to decrease noise energy according to [41].

The generated silent zone for the frequencies 63, 100, 160 and 250 Hz are visualized in Figs. 13 and 14 for active shielding and virtual sensing respectively. Both methodologies obtain a desired silent zone when the frequency is very low (63 and 100 Hz). At the frequencies of 160 and 250 Hz, attenuating the whole silent zone is not achieved. Previous section explains the reason why attenuation of active shielding is limited, but it is interesting that the virtual sensing method also does not obtain a significant difference in the achieved silent zone. It can be remarked that although the virtual sensing is the optimum at sensor locations based on an estimation, there is a similitude in the silent zone generated between the optimum at the virtual sensors locations and the optimum using active shielding at silent zone boundary.

Regarding the computational cost, it is one of the most important issues to decide which technique is convenient according to hardware limitation. Generalizing, the computational cost of an active shielding system is the computational cost of the controller specified for the number of sensors. It means, depends on the control algorithm, the size of the boundaries and Δ_x, which must achieve the restriction in Eq. (31). On the other hand, virtual sensing implies more operations by sensor location due to the transformation to the measured signals to obtain the estimated pressure at virtual sensor locations. The number of operation varies for each virtual sensing algorithm according to the transformation, e.g. it has different value for a Kalman filter [17] than a filter as the method in [16]. Using this analysis, it is evident that the active shielding methods are convenient when the sensor locations at boundary of silent zone are less than the needed by virtual sensors to cover the same area inside. Specifically, in the example shown in this section, active shielding method uses a multichannel controller with 12 sensors and 12 actuators. On the other hand, virtual sensing uses a multichannel control algorithm with 25 sensors and 12 actuators. Moreover, it requires the computational cost for the estimation of the error signal at this locations. Then, it is shown that the computational cost is satisfactorily reduced. A more detailed cases will be the subject of future work.

6. Conclusions

This paper showed a method for active shielding using the definition of implicit control. In Section 2, the implicit control concept was defined and explained through an example. This section ended up proposing a linear relation to ensure that the implicit control occurs. Then, the wave equation was discretized to obtain a discrete model. It yields a space state model which relates the pressure at the boundaries of a desired silent zone with the pressure inside it. Based on this, an active

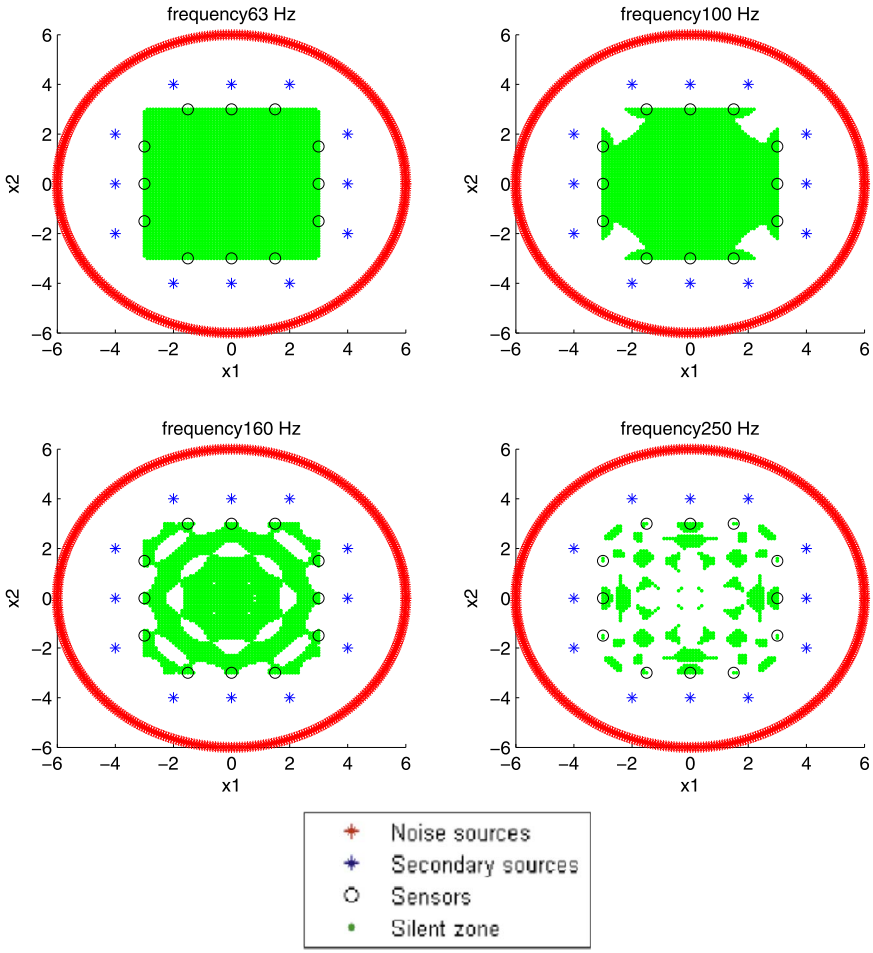

Fig. 13. Silent zone generated by an active shielding system.

shielding method was proposed. Later, the simulations presented the silent zone achieved for the proposed active shielding method. This result allows to conclude that if the finite difference approximation is valid, controlling the pressure at the boundaries of the desired silent zone implies controlling the pressure inside it. It means, it is an implicit control case. Moreover, it was concluded that applying an active control system to this case is an active shielding system, because it is only needed to control the pressure at the boundaries. It does not need more information to obtain the desired silent zone. From the simulated data, it can be inferred the same conclusion validating the theoretical approach for two and three dimensional systems. The simulations also showed that it happens for frequencies lower than 1/3 of the wave length in the proposed scheme. However, an even more detailed analysis shows that changing the frequency also produces a variation between the maximum value for Δ_x to achieve the implicit control. When the frequency is higher, the relation Δ_x/λ can be increased without loosing the attenuation effect inside the silent zone. Besides, the maximum acceptable relation between Δ_x/λ to achieve 90% of the desired silent zone with respect to the frequency was modeled by Eq. (31), which is the last contribution of this article.

This paper has shown basic concepts for the application of active shielding through implicit control. However, a deeper analysis allows a better understanding of this phenomenon and gives future applications. First, the statistical analysis in Section 4.3 produces Eq. (31), which will help the design an active shielding method. However, it does not show the theoretical reason why the distance affects the performance of the active shielding system in such a way. This relationship will be studied using an analytical analysis in future work. Second, when the sensors are located at pressure nodes there will be a problem for the controllers and may therefore limits the method's application. This will be analyzed in future work. Also, this article shows an approach for a free field environment, but it is not shown when surfaces interfere. The issue of this paper has an alternative solution using virtual sensing, in future works will be detailed the cases where it is convenient to use one or the other. For future works, implicit control will be evaluated under the non-free field conditions. Another problem is that the attenuation at the boundaries is not always obtained, usually because the actuators are less than the sensors. Thus, it is needed to obtain a method to decrease the number of actuators and sensors to control the boundary

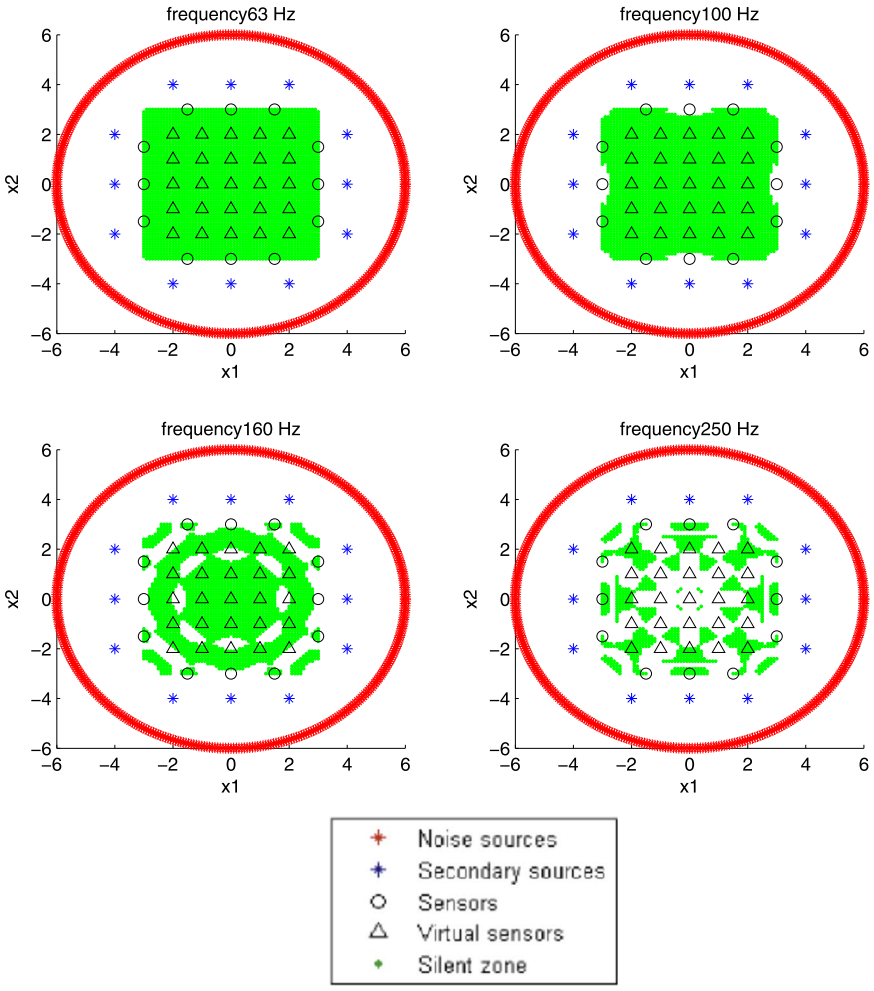

Fig. 14. Silent zone generated by a virtual sensing system.

locations. Besides, a massive multichannel control has problems converging. Consequently, it is recommended to focus future research on distributed and decentralized control.

Acknowledgment

We want to acknowledge to the Pontificia Universidad Javeriana for the support through the project "Control activo de un campo sonoro en tres dimensiones" with ID 6316. Also, we want to acknowledge to Colciencias (Departamento Administrativo de Ciencia, Tecnología e Innovación) for financing the Ricardo Quintana's doctoral student grant.

Appendix A. Three dimensional system

Analogous to the analysis shown in the Section 3, the three dimensional system obtains an active shielding method using implicit control. This case changes the wave equation, it uses $\nabla_{3D}(\cdot) := \frac{\partial^2 .}{\partial x_1^2} + \frac{\partial^2 .}{\partial x_2^2} + \frac{\partial^2 .}{\partial x_3^2}$ instead $\nabla_{2D}(\cdot)$. Notice that the third axis added is called x_3, i.e.:

$$\nabla_{3D}(p(X,t)) - d\frac{\partial p(X,t)}{\partial t} - \frac{1}{c^2}\frac{\partial^2 p(X,t)}{\partial t^2} = 0 \tag{A.1}$$

Subsequently, discretizing Eq. (A.1) using finite difference method yields:

$$p(x_{i,j,l}, k+1) = \gamma_{3,a}\Big[p(x_{i-1,j,l}, k) + p(x_{i+1,j,l}, k) + p(x_{i,j-1,l}, k) + p(x_{i,j+1,l}, k) + p(x_{i,j,l-1}, k) + p(x_{i,j,l+1}, k)\Big] + \gamma_{3,b}p(x_{i,j,l}, k) + \gamma_{3,c}p(x_{i,j,l}, k-1) \tag{A.2}$$

With:

$$\gamma_{3,a} = \frac{2c^2\Delta_t^2}{\Delta_x^2\left(dc^2\Delta_t + 2\right)} \tag{A.3}$$

$$\gamma_{3,b} = \left[\frac{4\left(\Delta_x^2 - 3c^2\Delta_t^2\right)}{\Delta_x^2\left(dc^2\Delta_t + 2\right)}\right] \tag{A.4}$$

$$\gamma_{3,c} = \left[\frac{dc^2\Delta_t - 2}{\left(dc^2\Delta_t + 2\right)}\right] \tag{A.5}$$

Then, the vector that contains the whole discrete locations inside a cubic silent zone $z_{3D}(k)$ is:

$$\bar{Z}_{j,l}(k) := \left[p(x_{1,j,l}, k) \quad p(x_{2,j,l}, k) \quad \cdots \quad p(x_{I,j,l}, k)\right]^T \tag{A.6}$$

$$\dot{Z}_l(k) := \left[\bar{Z}_{1,l}(k) \quad \bar{Z}_{2,l}(k) \quad \cdots \quad \bar{Z}_{J,l}(k)\right]^T \tag{A.7}$$

$$z_{3D}(k) := \left[\dot{Z}_1(k) \quad \dot{Z}_2(k) \quad \cdots \quad \dot{Z}_L(k)\right]^T \tag{A.8}$$

Also, the vector which contains the pressures at the boundary of this cube is:

$$\dot{u}_j(k) := \left[\bar{Z}_{j,1}(k) \quad \bar{Z}_{j,2}(k) \quad \cdots \quad \bar{Z}_{j,L}(k)\right]^T \tag{A.9}$$

$$\tilde{u}_{i,l}(k) := \left[p(x_{i,1,l}, k) \quad p(x_{i,2,l}, k) \quad \cdots \quad p(x_{i,J,l}, k)\right]^T \tag{A.10}$$

$$\bar{u}_i(k) := \left[\tilde{u}_{i,1}(k) \quad \tilde{u}_{i,2}(k) \quad \cdots \quad \tilde{u}_{i,L}(k)\right]^T \tag{A.11}$$

$$u_{3D}(k) := \left[\dot{Z}_0(k) \quad \dot{Z}_{L+1}(k) \quad \dot{u}_0(k) \quad \dot{u}_{J+1}(k) \quad \bar{u}_0(k) \quad \bar{u}_{I+1}(k)\right]^T \tag{A.12}$$

The next equation relates the vectors $z_{3D}(k)$ and $u_{3D}(k)$

$$\begin{bmatrix} z_{3D}(k+1) \\ z_{3D}(k) \end{bmatrix} = \begin{bmatrix} A_{3D} & \hat{A}_{3D} \\ \mathbb{I}_{IJL} & \mathbb{O}_{IJL,IJL} \end{bmatrix}\begin{bmatrix} z_{3D}(k) \\ z_{3D}(k-1) \end{bmatrix} + \begin{bmatrix} B_{3D} \\ \mathbb{O}_{IJL,2IJ+2JL+2IL} \end{bmatrix} u_{3D}(k) \tag{A.13}$$

Where the matrices are Where $\hat{A}_{3D} = \gamma_{3,c}\mathbb{I}_{IJL}$ and:

$$A_{3D} = \begin{pmatrix} \dot{A} & \gamma_{3,a}\mathbb{I}_{IJ} & \mathbb{O}_{IJ,IJ} & \cdots & & \cdots & \mathbb{O}_{IJ,IJ} \\ \gamma_{3,a}\mathbb{I}_{IJ} & \dot{A} & \gamma_{3,a}\mathbb{I}_{IJ} & \mathbb{O}_{IJ,IJ} & \ddots & & \vdots \\ \mathbb{O}_{IJ,IJ} & \gamma_{3,a}\mathbb{I}_{IJ} & \dot{A} & \gamma_{3,a}\mathbb{I}_{IJ} & \ddots & \ddots & \vdots \\ \vdots & \mathbb{O}_{IJ,IJ} & \ddots & \ddots & \ddots & \mathbb{O}_{IJ,IJ} & \vdots \\ \vdots & \ddots & \ddots & \ddots & \ddots & \ddots & \mathbb{O}_{IJ,IJ} \\ \vdots & & \ddots & \mathbb{O}_{IJ,IJ} & \gamma_{3,a}\mathbb{I}_{IJ} & \dot{A} & \gamma_{3,a}\mathbb{I}_{IJ} \\ \mathbb{O}_{IJ,IJ} & \cdots & \cdots & \cdots & \mathbb{O}_{IJ,IJ} & \gamma_{3,a}\mathbb{I}_{IJ} & \dot{A} \end{pmatrix} \tag{A.14}$$

With:

$$\dot{A} = \begin{pmatrix} \bar{A} & \gamma_{3,a}\mathbb{I}_I & \mathbb{O}_{I,I} & \cdots & & \cdots & \mathbb{O}_{I,I} \\ \gamma_{3,a}\mathbb{I}_I & \bar{A} & \gamma_{3,a}\mathbb{I}_I & \mathbb{O}_{I,I} & \ddots & & \vdots \\ \mathbb{O}_{I,I} & \gamma_{3,a}\mathbb{I}_I & \bar{A} & \gamma_{3,a}I_I & \ddots & \ddots & \vdots \\ \vdots & \mathbb{O}_{I,I} & \ddots & \ddots & \ddots & \ddots & \vdots \\ \vdots & \ddots & \ddots & \ddots & \ddots & \ddots & \mathbb{O}_{I,I} \\ \vdots & & \ddots & \mathbb{O}_{I,I} & \gamma_{3,a}\mathbb{I}_I & \bar{A} & \gamma_{3,a}\mathbb{I}_I \\ \mathbb{O}_{I,I} & \cdots & \cdots & \cdots & \mathbb{O}_{I,I} & \gamma_{3,a}\mathbb{I}_I & \bar{A} \end{pmatrix} \tag{A.15}$$

And the tridiagonal matrix $\bar{A} = [a_{m,n}]$ defines its components as:

$$a_{m,n} = \begin{cases} \gamma_{3,a} & \text{if } m = n \\ \gamma_{3,b} & \text{if } [m+1=n] \text{ and } [m-1=n] \\ 0 & \text{otherwise} \end{cases} \tag{A.16}$$

Besides, the relation between $z_{3D}(k+1)$ and $u_{3D}(k)$ is given by:

$$B_{2D} = [B_1 \quad B_2 \quad B_3 \quad B_4 \quad B_5]] \tag{A.17}$$

where:

$$B_1 = \begin{bmatrix} \gamma_{3,a}\mathbb{I}_{IJ} & \mathbb{O}_{(IJ),(IJ)} \\ \mathbb{O}_{(IJ),(IJ)} & \mathbb{O}_{(IJ),(IJ)} \\ \vdots & \vdots \\ \mathbb{O}_{(IJ),(IJ)} & \mathbb{O}_{(IJ),(IJ)} \\ \mathbb{O}_{(IJ),(IJ)} & \gamma_{3,a}\mathbb{I}_{IJ} \end{bmatrix} \tag{A.18}$$

$$B_2 = \begin{bmatrix} \bar{B}_2 & \mathbb{O}_{(IJ),J} & \cdots & & \mathbb{O}_{(IJ),J} \\ \mathbb{O}_{(IJ),J} & \bar{B}_2 & \mathbb{O}_{(IJ),J} & \cdots & \mathbb{O}_{(IJ),J} \\ \vdots & \ddots & \ddots & \ddots & \vdots \\ \vdots & \ddots & \ddots & \bar{B}_2 & \mathbb{O}_{(IJ),J} \\ \mathbb{O}_{(IJ),J} & \cdots & \cdots & \mathbb{O}_{(IJ),J} & \bar{B}_2 \end{bmatrix} \tag{A.19}$$

$$\bar{B}_2 = \begin{bmatrix} \hat{B}_2 & 0_{I,1} & \cdots & & \mathbb{O}_{I,1} \\ \mathbb{O}_{I,1} & \hat{B}_2 & \mathbb{O}_{I,1} & \cdots & \mathbb{O}_{I,1} \\ \vdots & \ddots & \ddots & \ddots & \vdots \\ \vdots & \ddots & \ddots & \hat{B}_2 & \mathbb{O}_{I,1} \\ \mathbb{O}_{I,1} & \cdots & \cdots & \mathbb{O}_{I,1} & \hat{B}_2 \end{bmatrix} \tag{A.20}$$

$$\hat{B}_2 = \begin{bmatrix} \gamma_{3,a} \\ \mathbb{O}_{(I-1),1} \end{bmatrix} \tag{A.21}$$

$$B_3 = \begin{bmatrix} \bar{B}_3 & \mathbb{O}_{(IJ),J} & \cdots & & \mathbb{O}_{(IJ),J} \\ \mathbb{O}_{(IJ),J} & \bar{B}_3 & \mathbb{O}_{(IJ),J} & \cdots & \mathbb{O}_{(IJ),J} \\ \vdots & \ddots & \ddots & \ddots & \vdots \\ \vdots & \ddots & \ddots & \bar{B}_2 & \mathbb{O}_{(IJ),J} \\ \mathbb{O}_{(IJ),J} & \cdots & \cdots & \mathbb{O}_{(IJ),J} & \bar{B}_3 \end{bmatrix} \tag{A.22}$$

$$\bar{B}_3 = \begin{bmatrix} \hat{B}_3 & \mathbb{O}_{I,1} & \cdots & & \mathbb{O}_{I,1} \\ \mathbb{O}_{I,1} & \hat{B}_3 & \mathbb{O}_{I,1} & \cdots & \mathbb{O}_{I,1} \\ \vdots & \ddots & \ddots & \ddots & \vdots \\ \vdots & \ddots & \ddots & \hat{B}_3 & \mathbb{O}_{I,1} \\ \mathbb{O}_{I,1} & \cdots & \cdots & \mathbb{O}_{I,1} & \hat{B}_3 \end{bmatrix} \tag{A.23}$$

$$\hat{B}_3 = \begin{bmatrix} \mathbb{O}_{(I-1),1} \\ \gamma_{3,a} \end{bmatrix} \tag{A.24}$$

$$B_4 = \begin{bmatrix} \bar{B}_4 & \mathbb{O}4_{(IJ),I} & \cdots & & \mathbb{O}_{(IJ),I} \\ \mathbb{O}_{(IJ),I} & \bar{B}_4 & \mathbb{O}_{(IJ),I} & \cdots & \mathbb{O}_{(IJ),I} \\ \vdots & \ddots & \ddots & \ddots & \vdots \\ \vdots & \ddots & \ddots & \bar{B}_4 & \mathbb{O}_{(IJ),I} \\ \mathbb{O}_{(IJ),J} & \cdots & \cdots & \mathbb{O}_{(IJ),I} & \bar{B}_4 \end{bmatrix} \tag{A.25}$$

$$\bar{B}_4 = \begin{bmatrix} \gamma_{3,a}\mathbb{I}_I \\ \mathbb{O}_{J(I-1),I} \end{bmatrix} \tag{A.26}$$

$$B_5 = \begin{bmatrix} \bar{B}_5 & \mathbb{O}_{(IJ),I} & \cdots & & \mathbb{O}_{(IJ),I} \\ \mathbb{O}_{(IJ),I} & \bar{B}_5 & \mathbb{O}_{(IJ),I} & \cdots & \mathbb{O}_{(IJ),I} \\ \vdots & \ddots & \ddots & \ddots & \vdots \\ \vdots & \ddots & \ddots & \bar{B}_5 & \mathbb{O}_{(IJ),I} \\ \mathbb{O}_{(IJ),J} & \cdots & \cdots & \mathbb{O}_{(IJ),I} & \bar{B}_5 \end{bmatrix} \tag{A.27}$$

$$\bar{B}_5 = \begin{bmatrix} \mathbb{O}_{J(I-1),I} \\ \gamma_{3,a}\mathbb{I}_I \end{bmatrix} \tag{A.28}$$

Thereby, a space state model can be written to express the behavior of pressure at the discrete locations in the silent zone. It is shown that the condition (5) is achieved also for a three dimensional system. Thus, if the desired silent zone is a parallelepiped, it can be obtained by controlling the noise at discrete location in the boundaries of this parallelepiped while it can be discretized as it was shown in this section. Consequently, the restrictions are given only by the finite difference method, which basically relates the frequency with Δ_x.

Appendix B. Control signal used in the simulation

In this article it is important to obtain the control signal at its maximum attenuation. The process to obtain the minimum attenuation at the sensor location is described below, similar as it is shown by [41]. It begins by describing the relation between the secondary source and error sensors signals, mathematically it is written as follows:

$$E_\iota(\omega) = D_\iota(\omega) + \sum_{j=1}^{\Lambda} H_{\iota,\lambda}(\omega)\nu_\lambda(\omega), \qquad i = 1, \ldots, N, \tag{B.1}$$

where $E_\iota(\omega) = F\{p(x_i, x_j, t)\}$ for two dimensional systems or $E_l(\omega) = F\{p(x_i, x_j, x_l, t)\}$ for three dimensional systems; ι expresses a different combination of i, j or i, j, l at boundary locations and its maximum value is the number of discrete locations at boundary of silent zone; $D_\iota(\omega)$ is the noise due to the primary source at sensor ι location; $H_{\iota,\lambda}(\omega)$ is the secondary path from the secondary source λ to the sensor ι; $\nu_\lambda(\omega)$ is the sound emitted by the secondary source λ; and Λ is the number of secondary sources. Eq. (B.1) can be written in matrix form as:

$$E(\omega) = D(\omega) + H(\omega)\nu(\omega). \tag{B.2}$$

With $E(\omega) = [E_1(\omega), E_2(\omega), \ldots, E_\Lambda(\omega)]^T$, $D(\omega) = [D_1(\omega), D_2(\omega), \ldots, D_\Lambda(\omega)]^T$, and $\nu(\omega) = [\nu_1(\omega), \nu_2(\omega), \ldots, \nu_\Lambda(\omega)]^T$ and defining the matrix:

$$H(\omega) = \begin{bmatrix} H_{1,1}(\omega) & H_{1,2}(\omega) & \cdots & H_{1,\Lambda}(\omega) \\ H_{2,1}(\omega) & H_{2,2}(\omega) & & H_{2,\Lambda}(\omega) \\ \vdots & \vdots & \ddots & \vdots \\ H_{\Lambda,1}(\omega) & H_{\Lambda,2}(\omega) & \cdots & H_{\Lambda,\Lambda}(\omega) \end{bmatrix} \tag{B.3}$$

Notice that it is assumed the number of sensors equal to Λ, it implies H to be a square matrix, which will be useful below. The control signal is obtained with the aim to minimize the energy of the sensors signals. It means:

$$\nu^*(\omega) = \underset{\nu(\omega)}{\operatorname{argmin}} E^{\mathcal{H}}(\omega)E(\omega) = -(H^{\mathcal{H}}(\omega)H(\omega))^{-1}H^{\mathcal{H}}(\omega)D(\omega), \tag{B.4}$$

Simplifying this result with the properties of square matrices, the control signal becomes:

$$\nu^*(\omega) = -H(\omega)^{-1}D(\omega), \tag{B.5}$$

References

[1] D. Guicking, On the invention of active noise control by paul lueg, J. Acoust. Soc. Am. 87 (5) (1990) 2251–2254, http://dx.doi.org/10.1121/1.399195.
[2] P. de Heering, Comments on 'on the invention of active noise control by paul lueg' [J. Acoust. Soc. Am. 87, 2251–2254 (1990)], J. Acoust. Soc. Am. 93 (5) (1993) http://dx.doi.org/10.1121/1.405819. (2989–2989).
[3] S. Kuo, M. Kuo, D. Morgan, Active Noise Control Systems: Algorithms and DSP Implementations, Wiley Series in Telecommunications and Signal Processing, Wiley, New York, United States of America., 1996.
[4] S.M. Kuo, D.R. Morgan, Active noise control: a tutorial review, Proc. IEEE 87 (6) (1999) 943–973, http://dx.doi.org/10.1109/5.763310.
[5] L.J. Eriksson, Development of the filtered-u algorithm for active noise control, J. Acoust. Soc. Am. 89 (1) (1991) 257–265, http://dx.doi.org/10.1121/1.400508.
[6] X.H. Yang, J. Van Niekerk, K.S. Parwani, A. Packard, B. Tongue, Attenuation of structurally generated interior noise through active control, in:

Proceedings of the American Control Conference, 199, 3, 1993, pp. 1–7.
[7] S. Lane, R. Clark, Active control of a reverberant enclosure using an approximate constant volume velocity source, in: Proceedings of the American Control Conference, vol. 4, 1998, pp. 2606–2610. http://dx.doi.org/10.1109/ACC.1998.703107.
[8] A. Sampath, R. Prasanth, R. Mehra, Robust interior noise control using system identification and linear matrix inequality (lmi) based control, in: Proceedings of the IEEE International Conference on Control Applications, vol. 1, 1998, pp. 679–683. http://dx.doi.org/10.1109/CCA.1998.728595.
[9] T. Yucelen, F. Pourboghrat, Active noise blocking: non-minimal modeling, robust control, and implementation, in: Proceedings of the American Control Conference, ACC'09, 2009, pp. 5492–5497. http://dx.doi.org/10.1109/ACC.2009.5160439.
[10] N.V. George, G. Panda, Advances in active noise control: a survey, with emphasis on recent nonlinear techniques, Signal Process. 93 (2) (2013) 363–377, http://dx.doi.org/10.1016/j.sigpro.2012.08.013.
[11] S. Elliott, C. Boucher, P. Nelson, The behavior of a multiple channel active control system, IEEE Trans. Signal Process. 40 (5) (1992) 1041–1052, http://dx.doi.org/10.1109/78.134467.
[12] S. Elliott, C. Boucher, Interaction between multiple feedforward active control systems, IEEE Trans. Speech Audio Process. 2 (4) (1994) 521–530, http://dx.doi.org/10.1109/89.326611.
[13] A. Montazeri, J. Poshtan, M.H. Kahaei, Optimal placement of loudspeakers and microphones in an enclosure using genetic algorithm, in: Proceedings of the 2003 IEEE Conference on Control Applications, CCA 2003, vol. 1, 2003, pp. 135–139. http://dx.doi.org/10.1109/CCA.2003.1223278.
[14] D. Li, M. Hodgson, Optimal active noise control in large rooms using a locally global control strategy, J. Acoust. Soc. Am. 118 (6) (2005) 3653–3661, http://dx.doi.org/10.1121/1.2114587.
[15] J. Garcia-Bonito, S.J. Elliott, C.C. Boucher, Generation of zones of quiet using a virtual microphone arrangement, J. Acoust. Soc. Am. 101 (6) (1997) 3498–3516, http://dx.doi.org/10.1121/1.418357 (URL ⟨http://scitation.aip.org/content/asa/journal/jasa/101/6/10.1121/1.418357⟩).
[16] A. Roure, A. Albarrazin, The remote microphone technique for active noise control, in: Proceedings of the Active 1999, Fort Lauderdale, 1999, pp. 1233–1244.
[17] C.D. Petersen, R. Fraanje, B.S. Cazzolato, A.C. Zander, C.H. Hansen, A kalman filter approach to virtual sensing for active noise control, Mech. Syst. Signal Process. 22 (2) (2008) 490–508, http://dx.doi.org/10.1016/j.ymssp.2007.06.007 (URL ⟨http://www.sciencedirect.com/science/article/pii/S0888327007001069⟩).
[18] D.J. Moreau, J. Ghan, B.S. Cazzolato, A.C. Zander, Active noise control in a pure tone diffuse sound field using virtual sensing, J. Acoust. Soc. Am. 125 (6) (2009) 3742–3755, http://dx.doi.org/10.1121/1.3123404 (URL ⟨http://link.aip.org/link/?JAS/125/3742/1⟩).
[19] D.P. Das, D.J. Moreau, B.S. Cazzolato, A nonlinear active noise control algorithm for virtual microphones controlling chaotic noise, J. Acoust. Soc. Am. 132 (2) (2012) 779–788, http://dx.doi.org/10.1121/1.4731227 (URL ⟨http://link.aip.org/link/?JAS/132/779/1⟩).
[20] C.D. Kestell, B.S. Cazzolato, C.H. Hansen, Active noise control in a free field with virtual sensors, J. Acoust. Soc. Am. 109 (1) (2001) 232–243, http://dx.doi.org/10.1121/1.1326950 (URL ⟨http://link.aip.org/link/?JAS/109/232/1⟩).
[21] J.M. Munn, B.S. Cazzolato, C.D. Kestell, C.H. Hansen, Virtual error sensing for active noise control in a one-dimensional waveguide: performance prediction versus measurement (l), J. Acoust. Soc. Am. 113 (1) (2003) 35–38, http://dx.doi.org/10.1121/1.1523386 (URL ⟨http://link.aip.org/link/?JAS/113/35/1⟩).
[22] J. Yuan, Virtual sensing for broadband noise control in a lightly damped enclosure, J. Acoust. Soc. Am. 116 (2) (2004) 934–941, http://dx.doi.org/10.1121/1.1768946 (URL ⟨http://link.aip.org/link/?JAS/116/934/1⟩).
[23] R. Quintana, L. Piroddi, D. Patino, Virtual sensing at low computational cost for active noise control, in: Proceedings of the INTER-NOISE and NOISE-CON Congress and Conference Proceedings, 250, 4, 2015, pp. 2989–2997. URL ⟨http://www.ingentaconnect.com/content/ince/incecp/2015/00000250/00000004/art00068⟩.
[24] N. Miyazaki, Y. Kajikawa, Head-mounted active noise control system with virtual sensing technique, J. Sound Vib. 339 (2015) 65–83, http://dx.doi.org/10.1016/j.jsv.2014.11.023 (URL ⟨http://www.sciencedirect.com/science/article/pii/S0022460X14009201⟩).
[25] M. Jessel, G. Mangiante, Active sound absorbers in an air duct, J. Sound Vib. 23 (3) (1972) 383–390, http://dx.doi.org/10.1016/0022-460X(72)90633-5 (URL ⟨http://www.sciencedirect.com/science/article/pii/0022460X72906335⟩).
[26] G. Canevet, Active sound absorption in an air conditioning duct, J. Sound Vib. 58 (3) (1978) 333–345, http://dx.doi.org/10.1016/S0022-460X(78)80042-X (URL ⟨http://www.sciencedirect.com/science/article/pii/S0022460X7880042X⟩).
[27] S. Uosukainen, Modified jmc method in active control of sound, Acta Acust. U. Acust. 83 (1) (1997) 105–112 (URL ⟨http://www.ingentaconnect.com/content/dav/aaua/1997/00000083/00000001/art00019⟩).
[28] S. Ise, A principle of sound field control based on the kirchhoff-helmholtz integral equation and the theory of inverse systems, Acta Acust. U. Acust. 85 (1) (1999) 78–87 (URL ⟨http://www.ingentaconnect.com/content/dav/aaua/1999/00000085/00000001/art00014⟩).
[29] N. Epain, E. Friot, Active control of sound inside a sphere via control of the acoustic pressure at the boundary surface, J. Sound Vib. 299 (3) (2007) 587–604, http://dx.doi.org/10.1016/j.jsv.2006.06.066 (URL ⟨http://www.sciencedirect.com/science/article/pii/S0022460X06005748⟩).
[30] M.L. Munjal, L.J. Eriksson, An analytical, one dimensional, standing wave model of a linear active noise control system in a duct, J. Acoust. Soc. Am. 84 (3) (1988) 1086–1093, http://dx.doi.org/10.1121/1.396694.
[31] B. Kwon, Y. Park, Active window based on the prediction of interior sound field: experiment for a band-limited noise, in: Proceedings of the Inter-Noise 2011, 2011.
[32] J. Loncaric, V.S. Ryaben'kii, S.V. Tsynkov, Active shielding and control of noise, SIAM J. Appl. Math. 62 (2) (2001) 563–596, http://dx.doi.org/10.1137/S0036139900367589 (URL ⟨http://dx.doi.org/10.1137/S0036139900367589⟩).
[33] H. Lim, S.V. Utyuzhnikov, Y.W. Lam, A. Turan, Multi-domain active sound control and noise shielding, J. Acoust. Soc. Am. 129 (2) (2011) 717–725, http://dx.doi.org/10.1121/1.3531933 (URL ⟨http://scitation.aip.org/content/asa/journal/jasa/129/2/10.1121/1.3531933⟩).
[34] H. Lim, S.V. Utyuzhnikov, Y.W. Lam, L. Kelly, Potential-based methodology for active sound control in three dimensional settings, J. Acoust. Soc. Am. 136 (3) (2014) 1101–1111, http://dx.doi.org/10.1121/1.4892934 (URL ⟨http://scitation.aip.org/content/asa/journal/jasa/136/3/10.1121/1.4892934⟩).
[35] V. Ryaben'kii, S. Utyuzhnikov, Differential and finite-difference problems of active shielding, Appl. Numer. Math. 57 (4) (2007) 374–382, http://dx.doi.org/10.1016/j.apnum.2006.05.002 (URL ⟨http://www.sciencedirect.com/science/article/pii/S0168927406000894⟩).
[36] V. Ryaben'kii, S. Tsynkov, S. Utyuzhnikov, Inverse source problem and active shielding for composite domains, Appl. Math. Lett. 20 (5) (2007) 511–515, http://dx.doi.org/10.1016/j.aml.2006.05.019 (URL ⟨http://www.sciencedirect.com/science/article/pii/S0893965906002072⟩).
[37] A. Loghmani, M. Danesh, M.K. Kwak, M. Keshmiri, Active structural acoustic control of a smart cylindrical shell using a virtual microphone, Smart Mater. Struct. 25 (4) (2016) 045020 (URL ⟨http://stacks.iop.org/0964-1726/25/i=4/a=045020⟩).
[38] J. Bay, Fundamentals of Linear State Space Systems, Electrical Engineering Series, WCB/McGraw-Hill, United States of America., 1999 (URL ⟨https://books.google.ca/books?id=vjoZAQAAIAAJ⟩).
[39] A.J. Antunes, R.C. Leal-Toledo, O.T. da Silveira Filho, E.M. Toledo, Finite difference method for solving acoustic wave equation using locally adjustable time-steps, Procedia Comput. Sci. 29 (2014) 627–636, http://dx.doi.org/10.1016/j.procs.2014.05.056 (URL ⟨http://www.sciencedirect.com/science/article/pii/S1877050914002336⟩).
[40] B. Hamilton, S. Bilbao, Optimised 25-point finite difference schemes for the three-dimensional wave equation, in: Proceedings of the International Conference on Acoustics, ICA 2016, 2016.
[41] S.J. Elliott, J. Cheer, Modeling local active sound control with remote sensors in spatially random pressure fields, J. Acoust. Soc. Am. 137 (4) (2015) 1936–1946, http://dx.doi.org/10.1121/1.4916274 (URL ⟨http://scitation.aip.org/content/asa/journal/jasa/137/4/10.1121/1.4916274⟩).